The George W. Woodruff School of Mechanical Engineering
Georgia Institute of Technology, Atlanta GA 30332-0405
Undergraduate Instructional Laboratories

TO: Michael Baldwin May 30, 2017

FROM: Abhay Dalmia, Evan Kaplan, & Alicia Lowrance ME 4056 Section A7

SUBJECT: Lab 1: Pitot-Static Probe and Thermal Anemometer

INTRODUCTION

The pitot-static probe and thermal anemometer experiment was performed at the Georgia Institute of Technology Mechanical Engineering Thermal Laboratory at the George W. Woodruff School of Mechanical Engineering on May 23, 2017. The objective of the lab was to become familiar with uncertainty tables and laboratory equipment, while characterizing air flow through a restriction using a pitot-static probe and thermal anemometer. This was done by measuring the velocity in the axial and transverse directions and the turbulent intensity in the transverse direction. The velocity was measured through digital and analog methods with the use of different types of manometers and a thermal anemometer.

APPARATUS AND UNCERTAINTY

Apparatus. The data collected in this experiment required the use of a Gunt Hamburg HM170 Wind Tunnel in conjunction with several manometers, a pitot-static probe, and a thermal anemometer. A static ring manometer, specifically a Gunt Hamburg Inclined Tube Manometer 0 mbar to 5 mbar with 0.05 mbar markings, and a wind speed indicator, specifically a Gunt Hamburg Inclined Tube Manometer 0 m/s to 28 m/s with 1 m/s markings, were used with the wind tunnel to establish constant conditions within the wind tunnel. Digitally measuring the velocity in the wind tunnel required a Gunt Hamburg Prandtl Tube pitot-static probe with a digital pressure gage, specifically an Ashcroft RXLdp Differential Pressure Transducer 1 mbar to 10 mbar, connected with a Fluke 70 III Digital Multimeter to record the voltage associated with the dynamic pressure of the wind tunnel. The analog velocity measurements required the Gunt Hamburg Prandtl Tube pitot-static probe connected with a wall-mounted manometer, specifically a Dwyer Duragage; -0.1” to 1.0” W.G. with 0.01” markings to measure the dynamic pressure of the air flow. The digital and analog measurements both required the use of a Gunt Hamburg 0 mm to 150 mm ruler with 5 mm markings to move the pitot-static probe to specific locations within the wind tunnel. Measuring the turbulent intensity required a thermal anemometer sensor and thermal anemometer DAQ, specifically a Dantec Dynamics A/S MiniCTA Anemometer Package Probe Type 55P16 and a Dantec Dynamics A/S MiniCTA Anemometer Software respectively. In addition, the thermal anemometer sensor required an Empire 30 cm Aluminum Comination Square ruler with 1 mm marking to track position within the wind tunnel. To measure the ambient conditions a thermometer was used to measure the temperature, specifically a VWR General Purpose Glass Thermometer, Cat. #89095-598; - 20 °C to 110 °C with 1 °C markings, to measure the

pressure a barometer was used, specifically O-N Ins. Aneroid Barometer; 500-780 mmHg with 5 mmHg markings. Table 1 lists the equipment used in this experiment and their associated uncertainties. The references for the uncertainty values are displayed below the table.

Table 1. Uncertainty of all utilized measurement devices.

Generic ID	Commercial ID	U_A	U_B	U_C
Induced Graft Wind Tunnel	Gunt Hamburg HM170 Educational Wind Tunnel	N/A	N/A	N/A
Static Ring Manometer	Gunt Hamburg Inclined Tube Manometer 0 mbar to 5 mbar w/ 0.05 mbar marking	0.025 mbar[(1)]	Neg.[(2)]	0.025 mbar[(1)]
Wind Speed Indicator	Gunt Hamburg Inclined Tube Manometer 0 m/s to 28 m/s w/ 1 m/s marking	0.5 m/s[(1)]	Neg. [(2)]	0.5 m/s[(1)]
Pitot-Static Probe w/ Digital Pressure Gage	Gunt Hamburg Prandtl Tube	0.23 m/s[(6)]	0.108 m/s[(6)]	0.25 m/s[(6)]
Digital Pressure Gage	Ashcroft RXLdp Differential Pressure Transducer 0 mbar to 10 mbar	N/A	0.93 Pa[(3)]	0.93 Pa[(3)]
Multimeter	Fluke 70 III Digital Multimeter	0.01 V[(1)]	N/A	0.01 V[(1)]
Pitot-Static Probe w/ wall-mounted Manometer	Gunt Hamburg Prandtl Tube	0.14 m/s[(6)]	Neg.[(2)]	0.14 m/s
Wall-Mounted Manometer	Dwyer Duragage: -0.1” to 1.0” W.G. w/ 0.01” marking	1.2 Pa[(1)]	Neg.[(2)]	1.2 Pa[(1)]
Ruler (Pitot Traverse)	Gunt Hamburg 0 mm to 150 mm w/ 5 mm marking	2.5 mm[(1)]	N/A	2.5 mm[(1)]
Thermal Anemometer Sensor	Dantec Dynamics A/S MiniCTA Anemometer Package Probe Type 55P16	N/A	0.12 m/s[(4)]	0.12 m/s[(4)]
Thermal Anemometer DAQ	Dantec Dynamics A/S MiniCTA Anemometer Software	N/A	0.37 m/s[(4)]	0.016 m/s[(4)]
Ruler (ThA Traverse)	Empire 30 cm Aluminum Comination Square w/ 1 mm marking	0.5 mm[(1)]	N/A	0.5 mm[(1)]
Thermometer	VWR General Purpose Glass Thermometer Cat. #89095-598; -20°C to 110°C w/ 1°C marking	0.5°C[(1)]	1°C[(5)]	1.1°C[(5)]
Barometer	O-N Ins. Aneroid Barometer; 500-780 mmHg w/ 5 mmHg marking	330 Pa[(1)]	N/A	330 Pa[(1)]

[(1)] By inspection; [(2)] Zeroing; [(3)] Calibration; [(4)] Dantec Dynamics (2004); [(5)] H-B Instrument Company (2009).; [(6)] Error Propagation Analysis

Uncertainty. Three types of uncertainty are found for each apparatus. Type A uncertainty, U_A, is the uncertainty associated with error by the user. Type B uncertainty, U_B, is uncertainty associated with the device. Type C uncertainty, U_C, is found by relating Type A and Type B uncertainties, using equation 1,

$$U_c = \sqrt{U_A^2 + U_B^2} \tag{1}$$

The U_A of the static ring manometer, wind speed indicator, multimeter, wall-mounted manometer, pitot traverse ruler, ThA traverse ruler, thermometer, and barometer is 0.025 mbar, 0.5 m/s, 0.01 V, 1.2 Pa, 2.5 mm, 0.5 mm, 0.5°C, and 330 Pa respectively, determined by taking half of the smallest graduation. The U_B of the static ring manometer, wind speed indicator, pitot-static probe with wall-mounted manometer, and wall-mounted manometer is negligible as each of these devices was zeroed immediately before the experiment began. The U_B of the digital pressure gage is 0.93 Pa, determined by taking 1% of its maximum reading recorded during the experiment. The U_B of the thermal anemometer sensor and the thermal anemometer DAQ is 0.12 m/s and 0.37 m/s respectively, determined by taking 1% of the sensor's and 3% of the DAQ's maximum mean velocity reading recorded during the experiment. The U_B of the thermometer is 1°C, determined by the uncertainty data provided by the device manufacturer: H-B Instrument Company, 2009. The thermal anemometer was improperly calibrated, so the resulting mean velocity values are off by a factor of 2, so all recorded mean velocity values are doubled, which all can be found in Attachment 2. None of the other data was affected.

The U_A of the pitot-static probe with digital pressure gage and the pitot-static probe with wall-mounted manometer is 0.23 m/s and 0.14 m/s respectively, while the U_B of the pitot-static probe with digital pressure gage is 0.108 m/s; all determined with error propagation analysis. Error propagation analysis for the velocity v was performed using the relation defined by Equation 2,

$$v = \sqrt{\frac{2P_D}{\rho}} \tag{2}$$

where P_D is the dynamic pressure and ρ is the density of air. For this lab, it was assumed that ρ has no uncertainty and hence, is a known constant (which is later proved to vary only by a negligible amount).

The pitot-static probe with digital pressure gage, used multimeter measurements of voltage and used Equation 3, to map voltages to dynamic pressures,

$$M_R[\text{V}] = 200P_D\ [\text{Pa}] \tag{3}$$

where M_R is the multimeter reading in volts and P_D is the corresponding dynamic pressure in pascals.

Hence, the U_B for the pitot-static probe comes only from the digital pressure gage. The Error Propagation Analysis for this is defined by Equation 4,

$$(U_v)_{B\,\text{Pitot-static with Pressure Gage}} = \sqrt{\left(\frac{\partial v}{\partial P_D} U_{P_G}\right)^2} = \sqrt{\frac{U_{P_G}^2}{2\rho P_D}} \tag{4}$$

where U_v is the systematic uncertainty of velocity values by the pitot-static probe with the digital pressure gage, U_{P_G} is the uncertainty of the digital pressure gage and P_D is the dynamic pressure reading.

Using the uncertainty of the digital pressure gage as 0.93 Pa, the density of air calculated as 1.68699 kg/m^2, and a minimum digital pressure gage value of 32.0 Pa, the systematic error is calculated as 0.108 m/s.

The U_A for the pitot-static probe comes only from the multimeter since the equipment was used for direct measurement. Combining Equations (2) and (3), the error propagation analysis as presented in Equation 5,

$$(U_v)_{A\,\text{Pitot-static with Pressure Gage}} = \sqrt{\left(\frac{\partial v}{\partial V} U_V\right)^2} = \sqrt{\frac{100 U_V^2}{\rho M_R}} \tag{5}$$

where U_v is the random uncertainty of velocity values by the pitot-static probe with the digital gage, ρ is the density of air, U_V is the uncertainty of the multimeter and M_R is the multimeter reading.

Using the uncertainty of the multimeter as 0.01 V and the minimum multimeter reading 0.160 V as MR, the random uncertainty is calculated as 0.23 m/s.

The pitot-static probe with the wall-mounted manometer also uses Equation 2 to calculate the velocity, but instead uses direct measurements from the wall-mounted manometer to do so. Hence, the random error of this measurement (U_A) is given in Equation 6,

$$(U_v)_{A\,\text{Pitot-static with Manometer}} = \sqrt{\left(\frac{\partial v}{\partial P_D} U_M\right)^2} = \sqrt{\frac{U_M^2}{2\rho P_D}} \tag{6}$$

where U_v is the random uncertainty in the velocity values produced by the pitot-static probe with the manometer, P_D is the dynamic pressure read by the manometer and U_M is the uncertainty of the manometer.

Using the manometer uncertainty as 1.2 Pa, air density as 1.68699, and minimum dynamic pressure reading of 32.0 Pa, it is calculated as 0.14 m/s.

PROCEDURE

The following procedure was used to complete the experiment. Using these steps, several data points were recorded and calculations were made as discussed in the following section.

1. Record the ambient room temperature and pressure readings.
2. Zero the static ring manometer and wall-mounted manometer.
3. Set the wind tunnel fan setting to 2.7.
4. Measure the initial values of the static ring manometer and wind speed indicator.
5. Zero the pitot-static probe.
6. Measure the voltage reading from the multimeter and the pressure reading from the wall-mounted manometer.
7. Move the pitot-static probe in 15 mm increments across the wind tunnel until 150 mm. Take the voltage and pressure readings at each increment.
8. Take final static ring manometer and wind speed indicators readings to ensure systematic consistency.
9. Position the thermal anemometer perpendicular to the air flow and at the 70 mm marker.
10. Measure the V_{mean} and V_{RMS}.
11. Move the thermal anemometer in 20 mm increments until 270 mm, measuring the V_{mean} and V_{RMS} at each increment.
12. Take two more V_{mean} and V_{RMS} measurements at points of interest, in this experiment 100 mm and 240 mm.

DATA ANALYSIS AND FINDINGS

Part 1. Flow of air through angled plates in a pitot-static probe to observe conservation of mass. (Pitot Probe)

The velocity profile and turbulent intensity through a restricted flow area with angled plates were investigated. Bernoulli's equation is used for the analysis of the velocity profile, so the assumptions for Bernoulli's equation needed to be met. These assumptions are the fluid is in steady state, the fluid is incompressible, the fluid acts along one streamline, and the fluid flow is inviscid. The steady state assumption can be made because the measurements from the fluid were recorded after the wind tunnel had been turned on for several minutes. At the time of measuring the data, nothing was changing as a function of time, inside the wind tunnel. Proof that the fluid is incompressible is shown within the data. The density at each position in the wind tunnel is calculated. The experimentally determined dynamic pressure at each point is used to calculate the density of the fluid at each point. Knowing the atmospheric pressure and the room temperature, the density is calculated using Equation 7, assuming that the air is an ideal gas,

$$\rho_{\text{air}} = \frac{P_{\text{atm}} - P_{\text{dynamic}}}{T_{\text{air}} \cdot \bar{R}} \tag{7}$$

where P_{atm} is the total pressure. P_{atm} is approximately equal to atmospheric pressure, P_{dynamic} is the dynamic pressure measured along the wind tunnel, $\bar{R}$ is the universal gas constant, T_{air} is the temperature of air, and ρ_{air} is the density of air.

Attachment 4 shows the density values for the air inside the wind tunnel change by less than 0.001 kg/m^3 during this experiment and can therefore be assumed to be incompressible. It can be assumed that each measurement was taken across the same streamline because all the measurements for Part I were taken in the center of the wind tunnel. In a long wind tunnel, air flows in only the axial direction at the center. Further, by showing that the solution to the boundary layer distance is small enough to be negligible, it can be shown that the air flow is inviscid. This done by solving the Blasius solution shown in Equation 8,

$$\delta = \frac{5x}{\sqrt{Re_x}} \tag{8}$$

where x is the characteristic length, which is equal to the length of the fin, and Re_x is the Reynolds number which can be solved using Equation 9.

$$Re_x = \frac{\rho v L}{\mu} \tag{9}$$

The density of air was calculated using the ideal gas equation as a function of pressure and temperature shown in Equation 10,

$$\rho = \frac{P}{\bar{R}T} \tag{10}$$

The density is calculated to be 1.17 kg/m^3. The characteristic length is found with simple geometry: $\frac{0.15}{\cos(26.6)} = 0.168$ m. The velocity of the inlet and outlet was measured as 6.5 m/s. The last variable is viscosity, found using an online viscosity calculator, which gave viscosity as $1.83 \cdot 10^{-5}$ kg/m-s [LMNO Engineering]. Finally, solving the two equations, the Reynolds number is $6.97 \cdot 10^4$ and the boundary layer length is equal to 3.18 mm. Because this length is much smaller than the width that the air travels through (a minimum of 146 mm), we can ignore the effects of friction. The flow is inviscid for the cross-section.

All the assumptions for Bernoulli's equation were satisfied, so the velocity is calculated at each point from the given pressures using Equation 2 and presented in Attachment 2. Attachment 2 shows that the velocity measurements calculated using the digital pressure gage were almost identical to the velocities calculated using the wall-mounted manometer. This shows that the precision of both devices is very high. There are slight differences between the measurements which could be related the digital pressure gage

requiring several devices to calculate the velocity. Each of these different devices adds uncertainty and sensitivity to the data. In this experiment, the manual manometer reading is preferred because it has an uncertainty of 0.14 m/s as opposed to the digital pressure gage with a higher uncertainty of 0.25m/s.

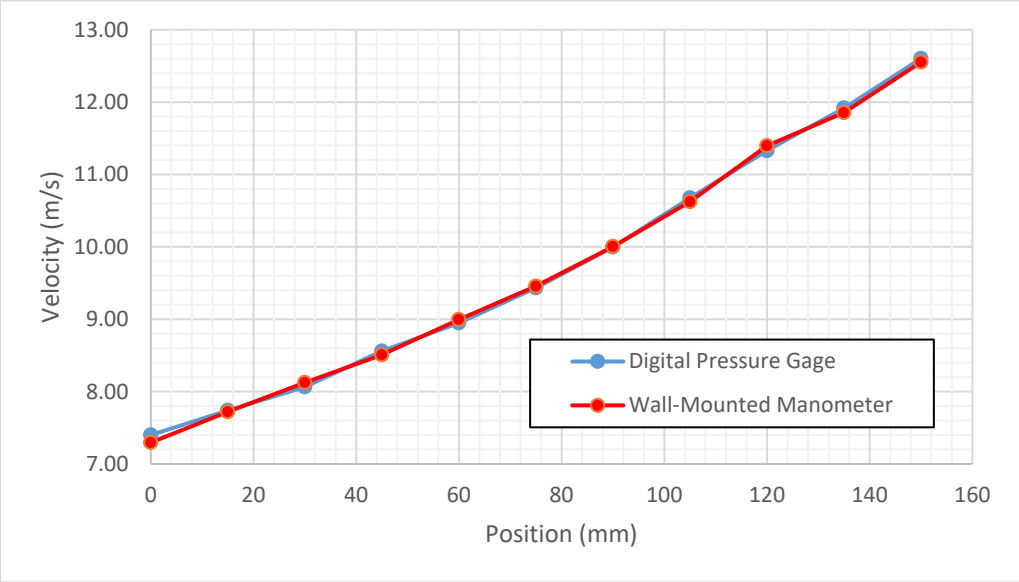

Figure 1. Plot of digital pressure gage and wall-mounted manometer axial velocity profile.

In Figure 1, the velocity of the air increases as the pitot-static probe moves farther from the origin. This is because the flow must satisfy the law conservation of mass. As the position gets farther from the origin, the cross-sectional area of the wind tunnel decreases. With the Bernoulli assumptions mentioned above, it should follow that the cross-sectional area multiplied by the axial velocity at each point should remain constant because the mass flow rate should theoretically remain constant.

In Figure 1, of the velocity profile is slightly curved upwards as expected. The cross-sectional area becomes smaller as the position increases, and area and velocity are inversely related per Equation 11,

$$Q = vA \tag{11}$$

where Q is the flow rate, v is the velocity of the fluid, and A is the cross-sectional area. Consequently, the curve is expected to be of the form f(x) = 1/x but reflected about a vertical line. The mass flow rate is calculated at each point, using Equation 11, of the streamline through the angled plate. This is shown in Figure 2.

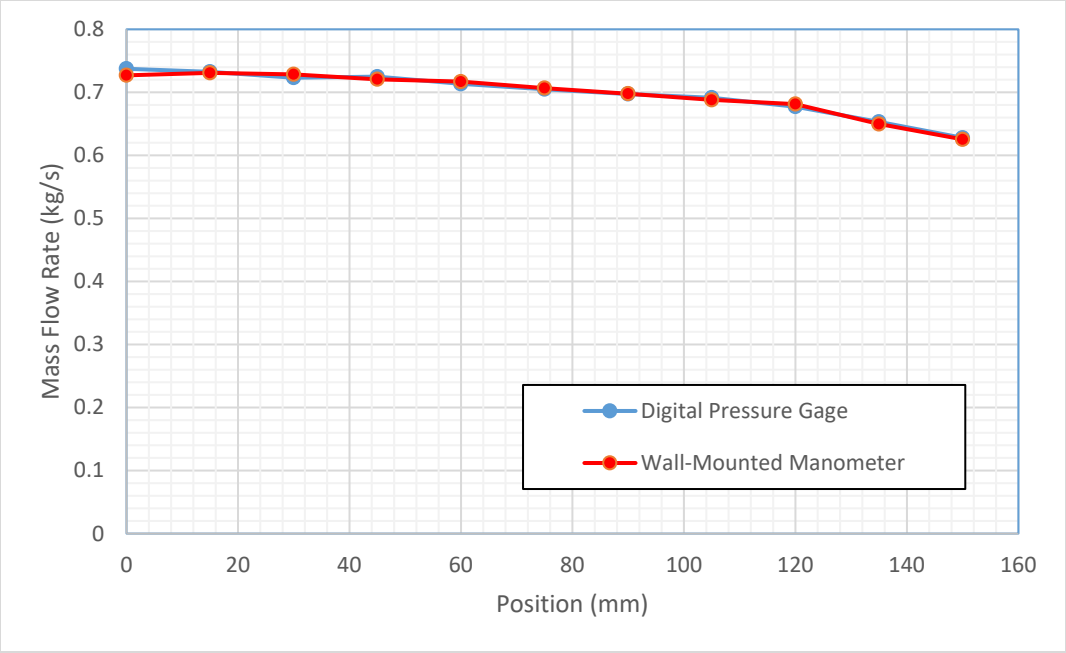

Figure 2. Plot of mass flow rate vs. axial location for wall-mounted manometer and digital pressure gage.

Figure 2 shows as the position increases, there is a decrease in the mass flow rate, so the law of was mass conservation is not conserved. This is due to the non-uniform velocity distribution within the wind-tunnel. The reason for this is that the inviscid assumption is not perfect and there is friction acting on the fluid. Thus, as the fluid moves along the wind tunnel, there is energy lost to viscous frictional forces against the wall creating a slower wind velocity than expected. Additionally, a perfect velocity distribution assumes perfect symmetry and construction of the wind tunnel with the angled plates, which is unreasonable to guarantee. Due to asymmetry of the chamber and imperfect wind generation inside the tunnel, a non-uniform velocity distribution is created. Using velocity to calculate mass flow rate shows a decrease in the mass flow rate as the air moves along the wind tunnel. Evidence that there is a varying velocity along the cross section of the wind tunnel is shown in Figure 3, which shows the wind velocity across the cross section at the end of the fins. This figure is for Part 2 of the experiment, but supports findings from Part 1. In Figure 3, velocity decreases drastically near the edges of the wall. In comparison with the width of the tunnel, the 3 mm boundary layer becomes too large to ignore the inviscid effects. This comparison gets more drastic as the width of the tunnel decreases. This can also be seen in Figure 2. The mass flow rate seems to be decreasing at a higher rate as the position increases because as the position increases, the width of the tunnel decreases and the boundary layer impacts the mass flow rate of the fluid.

In this experiment, the flow of the fluid within the plates remains in the laminar region. The Reynolds number is calculated for each point in the pitot-static probe measurement in Attachment 5, using Equation 9. The critical Reynolds number observed for this experiment is $5 \cdot 10^5$, that of a flow over a flat

plane. As the Blasius solution yields a boundary layer of 3.18 mm, which is much smaller than the width of the wind tunnel, the flow is largely external and hence can be estimated as such. The flow over the angled plane, then, is considered similar to that of external flow over a plate.

This evidence is also supported by the velocity profile determined in Part 2 of this experiment. The edge of the angled plate is expected to have the most turbulence. Turbulence is a function of dynamic viscosity, air density, characteristic length, and air velocity. The air density and dynamic viscosity changed negligibly over the longitudinal direction of the wind tunnel, so then turbulence is largely only a function of velocity. The highest turbulence is found at the end of the angled plates, where velocity is greatest, seen in Figure 1. This region is mapped in Part 2 and turbulent intensities across this region were found to be <5%. This is in the laminar region of the flow.

The center channel through the angled plates operated in the laminar region, so the results are not expected to be affected by this phenomenon; however, turbulence is a gradient rather than a set point. There are still minimal amounts of turbulence that disturbs the velocity profile and further explains the unequal distribution of velocity and slight deviation from continuity.

Part 2. Flow Profile across wind tunnel with angled plates obstruction. (Thermal Anemometer)

The flow regime and velocity profile, based upon the thermal anemometer readings, were investigated in the second part of the experiment. Figure 3 presents the experimental data for the mean velocity versus position to establish the velocity profile as well as the calculated turbulent intensity for the flow based upon the experimental root mean square (RMS) velocity. The turbulent intensity is calculated using Equation 12,

$$TI = \frac{v_{RMS}}{\bar{v}} \tag{12}$$

where turbulent intensity is simply the ratio of the RMS velocity to the mean velocity. The turbulent intensity is used to establish the flow regime with the rule that any flow with a TI < 5% is laminar and a TI > 5% is turbulent. The turbulent intensity is an appropriate indicator of flow regime because the RMS velocity is calculated with Equation 13,

$$v_{RMS} = \sqrt{\frac{\sum_i (v_i - \bar{v})^2}{N}} \tag{13}$$

where N is the number of samples taken at the same data point. This RMS velocity equation targets the variance between the mean velocity and actual velocity which is vital in establishing the flow regime because the more velocity fluctuation there is, the more turbulent the flow regime. This is evident in the Equation 12 as the RMS velocity is in the numerator, so the more variation in the flow's velocity, the higher the TI.

For this particular flow, Figure 3 indicates the flow is laminar between the plates but becomes less

laminar near the angled plates and turbulent outside the plates. This is evident by the turbulent intensity between -60 and 60 mm ranging between 1.73% and 3.81% and the largest values for the turbulent intensity located at -60 and 60 mm. Beyond the -60 and 60 mm positions, the turbulent intensity spikes to values almost three times the turbulent intensity within the plates, indicating turbulent flow. The flow becomes more turbulent near the plates because viscous effects are more prominent in the boundary layer; consequently, the boundary layer is very small at 3.18 mm, so the turbulent effect is only evident at the plates.

In this experiment, the velocity of a constricted air flow was measured with a thermal anemometer and pitot-static probe. Both devices proved effective in establishing an appropriate velocity profile and identifying a flow regime. The thermal anemometer, however, has some advantage over the pitot-static probe. Firstly, the combined uncertainty of the thermal anemometer is lower than the pitot-static probe combined uncertainty by 0.02 m/s. In addition, the thermal anemometer reaches steady state almost instantaneously because the wire diameter at the end of the anemometer is smaller than that of a human hair. This instantaneous steady state allows for many more repeated readings to be taken at each position within the air flow. The larger data set allows for the mean velocity to be taken experimentally, giving a more accurate calculated Reynold's number as the equation calls for the mean velocity, not the instantaneous velocity of the air flow. Lastly, the experimental mean velocity and breadth of data points allows for the RMS velocity to be accurately calculated, which is fundamental to finding the turbulent intensity. As turbulent intensity is the more appropriate method for determining flow regime of an unconventional air flow (angled plates), the thermal anemometer is the better device for experimentally determining the velocity profile and flow regime of the air flow.

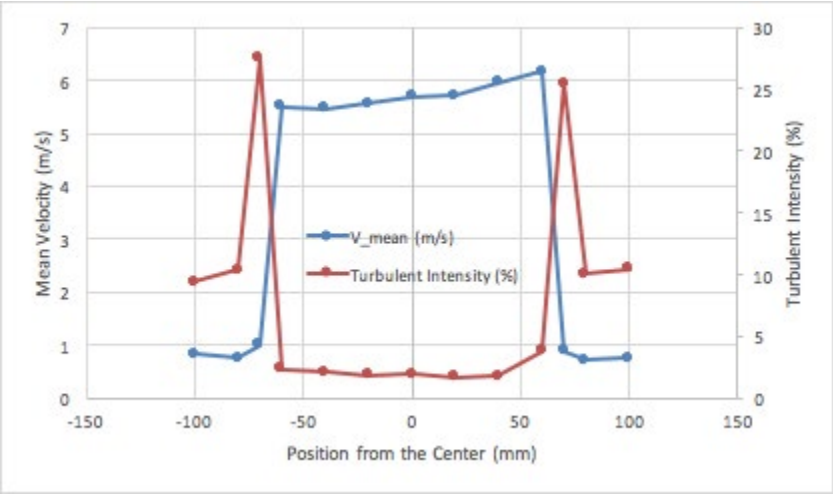

Figure 3. Plot of the thermal anemometer mean velocity reading and calculated turbulent intensity from the thermal anemometer RMS velocity reading.

CLOSURE

Several trends are determined, with regard to flow rate, in this experiment. From Part 1, the flow rate along the longitudinal direction through angled plates was investigated to determine continuity. Two different methods of measurements were used to compare and validate them, as shown in Figure 1. Both yielded very close results with RMS error between the two at less than 0.19 m/s. Based on this data, continuity was mostly observed with an average flow rate of 0.59 m^3/s. However, there were slight difference to flow rate, especially near plate edges, that is explained by non-uniform velocity distributions through the region, explained by slight differences in wind tunnel construction and random turbulent effects, as shown in Figure 2. Based on the results, other assumptions made in this Part 1 were substantiated, including treating air as an ideal gas and Bernoulli's equation for calculating velocities.

In the Part 2, the velocity profile and turbulence were investigated across the cross-section of the angled plane. The data supports the Blasius solution for boundary layer as the flow through the central region is mostly flat and not parabolic, suggesting that the boundary layer was minimal and viscous affects were negligible. The effect of change in geometry/obstruction on turbulence was also determined. At the edge of the angled plates, the turbulent intensity rose to 25%. This is well above the 5% threshold for turbulent flow. Between the wind tunnel wall and the angled plate, the turbulent intensity of the flow averages at 12%.

REFERENCES

Bruce R. Munson, Theodore H. Okiishi, Wade W. Huebsch, and Alric P. Rothmayer, *Fundamentals of Fluid Mechanics*, 7th Edition, John Wiley and Sons, 2013.

Dantec Dynamics A/S, 2004, Publication No. 9040U6162, Skovlunde, Denmark, 23 January 2004.

"Gas Viscosity Calculator." The Fluid Flow Calculations Website. LMNO Engineering, Research, and Software, Ltd., n.d. Web. 28 May 2017.

H-B Instrument Company, 2009, "Traceable Thermometer Statement (Calibration Certificate #2448.01) against ISO/IEC 17025:2005 and ANSI/NCSL Z540-1-1994," Collegeville, PA.

Attachment 1. Experimental and setup conditions.

Experimental Conditions								
Ambient Conditions:								
Ambient Pressure:		735	mmHg		97.99195	kPa		
Room Temperature		19	C		292	K		
Air Density:		1.168699	kg/m3					
Dynamic Viscosity		1.83E-05	kg/m-s					
Gas constant R:		287			J/kg-K			
Instrument Dimensions								
Duct Width		292	mm		Duct Height		292	mm
Angled Plate:	Angle	26.6	degrees		Length		150	mm
CS Area:	A_0	0.0853	m^2		A_f		0.0426	m^3
Recurring Data and Calculations								
Fan Setting		2.7						
Vind	Offset	0	m/s		P_SR	Offset	0	mbar
	Start	6.5	m/s			Start	0.25	mbar
	End	6.5	m/s			End	0.25	mbar
	Mean	6.5	m/s			Mean	25	Pa
Reynolds Number								
	Re	6.97E+04			bound lay	3.18E-03		
Mass Flow Rate								
	m_dot	0.648	kg/s					

Attachment 2. Pitot-static probe traverse tabulated and calculated data.

x [mm]	Area [m^2]	E_DPG [V]	Delta_P DPG [Pa]	V_DPG [m/s]	Delta_P Manometer [in WC]	Delta_P Manometer [Pa]	V Manometer [m/s]
0	0.0853	0.16	32.0	7.40	0.125	31.105	7.2958985
15	0.0810	0.175	35.0	7.74	0.14	34.8376	7.7212532
30	0.0767	0.19	38.0	8.06	0.155	38.5702	8.1243687
45	0.0725	0.214	42.8	8.56	0.17	42.3028	8.5084066
60	0.0682	0.234	46.8	8.95	0.19	47.2796	8.9949878
75	0.0639	0.26	52.0	9.43	0.21	52.2564	9.4565653
90	0.0597	0.292	58.4	10.00	0.235	58.4774	10.003632
105	0.0554	0.333	66.6	10.68	0.265	65.9426	10.622989
120	0.0512	0.375	75.0	11.33	0.305	75.8962	11.396558
135	0.0469	0.415	83.0	11.92	0.33	82.1172	11.854432
150	0.0426	0.464	92.8	12.60	0.37	92.0708	12.552338

Attachment 3. Thermal Anemometer traverse tabulated and calculated data.

L [mm]	y [mm]	V_mean [m/s]	V_mean_actual [m/s]	V_rms [m/s]	I [%]
70	-100	0.836	1.672	0.157	9.39
90	-80	0.758	1.516	0.157	10.36
100	-70	0.998	1.996	0.548	27.45
110	-60	5.509	11.018	0.261	2.37
130	-40	5.47	10.94	0.232	2.12
150	-20	5.566	11.132	0.211	1.90
170	0	5.69	11.38	0.225	1.98
190	20	5.703	11.406	0.197	1.73
210	40	5.958	11.916	0.208	1.75
230	60	6.169	12.338	0.470	3.81
240	70	0.897	1.794	0.457	25.47
250	80	0.719	1.438	0.144	10.01
270	100	0.757	1.514	0.158	10.44

Attachment 4. Density calculation along several points of the pitot-static probe.

x	Delta_P DPG	P_total	P_static	Density
[mm]	[Pa]	Pa	Pa	kg/m^3
0	32.0	97991.95	97960.0	1.168317
15	35.0	97991.95	97957.0	1.168281
30	38.0	97991.95	97954.0	1.168246
45	43.0	97991.95	97949.2	1.168188
60	47.0	97991.95	97945.2	1.168141
75	52.0	97991.95	97940.0	1.168079
90	58.0	97991.95	97933.6	1.168002
105	67.0	97991.95	97925.4	1.167905
120	75.0	97991.95	97917.0	1.167804
135	83.0	97991.95	97909.0	1.167709
150	93.0	97991.95	97899.2	1.167592

Attachment 5. Reynold's Number calculated along the flow of the pitot-static probe.

x	V Manometer	Reynold's Number
[mm]	[m/s]	
0	7.295898505	78112.271
15	7.721253215	82666.257
30	8.124368739	86982.144
45	8.508406643	91093.779
60	8.994987782	96303.275
75	9.456565275	101245.07
90	10.00363203	107102.15
105	10.62298857	113733.18
120	11.39655779	122015.27
135	11.85443193	126917.42
150	12.55233841	134389.43